ISSN 1674-1056
http://cpb.iphy.ac.cn
http://iopscience.iop.org/cpb
中国物理 B
Chinese Physics
中国物理
Chinese Physics B

Generation of Mathieu beams using angular pupil modulation

Zhijun Ren(任志君), Jinping He(何晋平), Yile Shi(施逸乐)

Citation: Chin. Phys. B . 2018, 27(12): 124201. **doi:** 10.1088/1674-1056/27/12/124201
Journal homepage: http://cpb.iphy.ac.cn; http://iopscience.iop.org/cpb

What follows is a list of articles you may be interested in

Terahertz two-pixel imaging based on complementary compressive sensing

Yuye Wang(王与烨), Yuchen Ren(任宇琛), Linyu Chen(陈霖宇), Ci Song(宋词), Changzhao Li(李长昭), Chao Zhang(张超), Degang Xu(徐德刚), Jianquan Yao(姚建铨)

Chin. Phys. B . 2018, 27(11): 114204. **doi:** 10.1088/1674-1056/27/11/114204

Further analysis of scintillation index for a laser beam propagating through moderate-to-strong non-Kolmogorov turbulence based on generalized effective atmospheric spectral model

Jing Ma(马晶), Yu-Long Fu(付玉龙), Si-Yuan Yu(于思源), Xiao-Long Xie(谢小龙), Li-Ying Tan(谭立英)

Chin. Phys. B . 2018, 27(3): 034201. **doi:** 10.1088/1674-1056/27/3/034201

(3+1)-dimensional localized self-accelerating Airy elegant Ince-Gaussian wave packets and their radiation forces in free space

Dongdong Li(李冬冬), Xi Peng(彭喜), Yulian Peng(彭玉莲), Liping Zhang(张丽萍), Xingyu Chen(陈星宇), Jingli Zhuang(庄经立), Fang Zhao(赵方), Xiangbo Yang(杨湘波), Dongmei Deng(邓冬梅)

Chin. Phys. B . 2017, 26(12): 124202. **doi:** 10.1088/1674-1056/26/12/124202

Characteristics of photonic nanojets from two-layer dielectric hemisphere

Yunyue Liu(刘昀玥), Xianchao Liu(刘贤超), Ling Li(李玲), Weidong Chen(陈卫东), Yan Chen(陈艳), Yuerong Huang(黄跃容), Zhengwei Xie(谢征微)

Chin. Phys. B . 2017, 26(11): 114201. **doi:** 10.1088/1674-1056/26/11/114201

Near-field characteristics of highly non-paraxial subwavelength optical fields with hybrid states of polarization

Rui-Pin Chen(陈瑞品), Teng-Yue Gao(高腾跃), Khian-Hooi Chew(周健辉), Chao-Qing Dai(戴朝卿), Guo-Quan Zhou(周国泉), Sai-Ling He(何赛灵)

Chin. Phys. B . 2017, 26(10): 104202. **doi:** 10.1088/1674-1056/26/10/104202

Generation of Mathieu beams using angular pupil modulation*

Zhijun Ren(任志君)[1,†], Jinping He(何晋平)[2], and Yile Shi(施逸乐)[1]

[1] Key Laboratory of Optical Information Detecting and Display Technology, Zhejiang Normal University, Jinhua 321004, China
[2] National Astronomical Observatories/Nanjing Institute of Astronomical Optics & Technology, Chinese Academy of Sciences, Nanjing 210042, China

(Received 9 July 2018; revised manuscript received 4 September 2018; published online 10 November 2018)

By using an amplitude-type spatial light modulator to load angular spectrum of Mathieu function distribution along a narrow annular pupils, the Durnin's experimental setup is extended to generate various types of Mathieu beams. As a special type of Mathieu beams, Bessel beams are also generated using this optical setup. Furthermore, the optical morphology of the Mathieu beams family are also presented and analyzed.

Keywords: diffraction-free beams, Mathieu beams, angular modulation, spatial light modulator

PACS: 42.25.Bs, 42.30.Kq, 42.30.Lr, 42.60.Jf **DOI:** 10.1088/1674-1056/27/12/124201

1. Introduction

Since the generation of Bessel beams in 1987,[1] diffraction-free beams, which can propagate over an extended distance with an invariant transverse profile, have attracted much attention because of their especially useful value in some application fields, such as laser surgery, optical coherence tomography, and optical trapping.[2,3] Each diffraction-free beam is a fundamental solution of the wave equation. The most familiar example of diffraction-free beams is the plane wave, which is the solution of the wave equation in Cartesian coordinates. Bessel beams are the fundamental solutions of the wave equation in circular cylindrical coordinates. In elliptic cylindrical coordinates, Gutiérrez–Vega found another special solution of wave equation, which is the Mathieu function. Accordingly, diffraction-free Mathieu beams are also introduced and researched in theory.[4,5]

The propagation-invariant nature of the transverse field profile of diffraction-free beams is a result of their cone-like angular spectrum: all plane wave components have equal longitudinal wavenumber, which can be described by the Dirac delta function $\delta(|k|-k_t)$. Here, we will extend the original experiment of Durnin to create an annular pupil aperture in the Fourier plane with arbitrary azimuthal amplitude components. We know that by using an annular pupil in focal plane of Fourier transform lens illuminated by a collimated laser beam, diffraction-free Bessel beams can be generated after Fourier-transform lens.[1] Compared with Bessel beams generation, Mathieu beams generation can be especially difficult because the annular slit required in modulation profiles is the spectra distribution with angular Mathieu functions. To generate Mathieu beams using the experimental setup of Durnin, researchers had to introduce several approximate methods. For example, Gutiérrez–Vega make a one-dimensional (1D) Gaussian aperture and optimized its parameters to match the angular spectra of Mathieu functions to approximately generate zero-order Mathieu beams.[6] Compared with classical two-dimensional (2D) radial Gaussian beams, 1D Gaussian beams in Ref. [6] are also difficult to obtain. In 2008, Anguiano-Morales generated a field distribution that is close to the diffraction-free Mathieu beam by using a combination of an axion and amplitude mask with two circular sectors of 70°.[7] In Ref. [8], Florian even generated sectioned Bessel beams by blocking sections of a beam's angular spectrum, which are a kind of quasi diffraction-free beams similar to optical distribution of Mathieu beams.

A spatial light modulator (SLM) is an important element to precisely modulate the phase or amplitude of the beam wavefront. To generate Mathieu beams, we extend the original experimental setup of Durnin[1] to generate ring slit apertures with amplitude distribution of angular Mathieu function using amplitude-type SLM placed in the front focal plane of a Fourier-transform lens. Hence, we obtain a family of ideal Mathieu beams after lens by accurately generating angular Mathieu function. The optical characteristics of Mathieu beams are subsequently analyzed.

2. Theory

We begin our analysis on Mathieu beams generation with the scalar wave equation $(\nabla^2+k^2)\boldsymbol{E}(\boldsymbol{r})=0$, where r is the position vector and k is the wavenumber. We assume a solution of the form $\boldsymbol{E}(\boldsymbol{r})=U(x,y)Z(z)$, thus separating the wave equation into two equations, which is

$$\left[\frac{\mathrm{d}^2}{\mathrm{d}z^2}+k_z^2\right]Z(z)=0, \tag{1}$$

$$\left[\nabla^2+k_t^2\right]U(x,y)=0, \tag{2}$$

*Project supported by the National Natural Science Foundation of China (Grant No. 11674288).
†Corresponding author. E-mail: renzhijun@zjnu.cn
© 2018 Chinese Physical Society and IOP Publishing Ltd

where $k^2 = k_t^2 + k_z^2$, k_t and k_z is radial and axial wavenumber, respectively. Equation (1) is the Harmonic equation whose solution is $Z(z) = \exp(\mathrm{i}k_z z)$. The elliptic coordinates (u, v, z) are defined by Cartesian coordinates (x, y, z) according to the transformation $(x + \mathrm{i}y) = f\cosh(u + \mathrm{i}v)$. By introducing the scale factors in elliptic coordinates $s \equiv s_u = s_v = f\sqrt{\cosh 2u - \cos 2v} = f\sqrt{\frac{1}{2}(\cosh 2u - \cos 2v)}$, equation (2) can be written as[8–10]

$$\left[\frac{\partial^2}{\partial u^2} + \frac{\partial^2}{\partial v^2} + \frac{f^2 k_t^2}{2}(\cosh 2u - \cos 2v)\right] U_e(u, v) = 0, \quad (3)$$

where f is the semi-focal distance of ellipse, the radial variable $u \in (0, \infty)$ and angular variable $v \in (0, 2\pi)$. To use the method of separation of variables, we assume a solution of the form $U_e(u, v) = R(u)S(v)$. Substitution of $U_e(u, v)$ into Eq. (3) yields the following form of Mathieu differential equations

$$\left[\frac{\partial^2}{\partial u^2} - (c - 2q\cosh 2u)\right] R(u) = 0, \quad (4)$$

$$\left[\frac{\partial^2}{\partial v^2} + (c - 2q\cos 2v)\right] S(v) = 0, \quad (5)$$

where c is separation constant. A dimensionless parameter q carries beam information by $q = (f^2/4)k_t^2$. Equations (4) and (5) are named as radial and angular Mathieu equations, respectively. Notice that equation (4) can transform into Eq. (5) with the replacement $u \Leftrightarrow \mathrm{i}v$. Consequently, the solution of the scalar wave equation in elliptic coordinates can be written as follows:[9–11]

$$E = \begin{pmatrix} C_m \\ S_m \end{pmatrix} \begin{pmatrix} \mathrm{Je}_m(u, q) \\ \mathrm{Jo}_m(u, q) \end{pmatrix} \begin{pmatrix} \mathrm{ce}_m(v, q) \\ \mathrm{se}_m(v, q) \end{pmatrix} \exp(\mathrm{i}k_z z), \quad (6)$$

where $\mathrm{Je}_m(u, q)$ and $\mathrm{ce}_m(v, q)$ are the m-th-order even radial and angular Mathieu function, respectively. Whereas $\mathrm{Jo}_m(u, q)$ and $\mathrm{se}_m(v, q)$ are the m-th-order odd radial and angular Mathieu functions, respectively. C_m and S_m are the balancing constants to ensure each even and odd mode carries equal power, and both do not influence the distribution of beams, hence they are usually omitted. The propagation term $\exp(\mathrm{i}k_z z)$ only introduces a global phase on the Mathieu beams.

Equation (6), derived from Eq. (1), represents a transverse Mathieu field distribution propagating in the z direction with a phase velocity $v_\mathrm{p} = w/k_z$. Since the amplitude distribution is not related to z, equation (6) represents an ideal propagation-invariant beam that can be described by the known Mathieu functions. Similar with the plane wave solution of wave equation in Cartesian coordinate and the Bessel solution in circular cylindrical coordinates of wave equation, equation (6) shows another fundamental solution of wave equation in elliptic cylindrical coordinates.

On the basis of Eq. (6), we plot the transverse intensity distributions of the even-parity Mathieu beams of the first kind with parameters $m = 0$, 1, 2, 3 and $q = 0$, 15, 30, 45 (as show in Fig. 1). Each stimulating and recording photo (including that in Figs. 1, 4, and 5) shows an area size of 1 mm × 1 mm in this study. When $m = 0$ in Eq. (6), their fundamental solutions are the angular Mathieu function $\mathrm{ce}_0(v, q)$ and radial Mathieu function $\mathrm{Je}_0(u, q)$. When constant coefficient is ignored, equation (6) can be referred to as the zero-order Mathieu beams

$$Ze_0 = \mathrm{Je}_0(u, q)\mathrm{ce}_0(v, q)\exp(\mathrm{i}k_z z). \quad (7)$$

As shown in Figs. 1(a)–1(d), the zero-order Mathieu beams' distribution is characterized by the ellipticity parameter q. With increasing q, the elliptical main lobes of zero-order Mathieu beams become increasingly flat. Radial unsymmetrical zero-order Mathieu beams transform into radial symmetry zero-order Bessel beams when $q = 0$, as shown in Figs. 1(a)–1(d). The central main lobes of the zero-order Bessel beams are circular spots. Similar to the Airy beams being a special type of the Weber beams,[12] the circularly symmetric zero-order Bessel beams are a special case of zero-order Mathieu beams when $q = 0$.

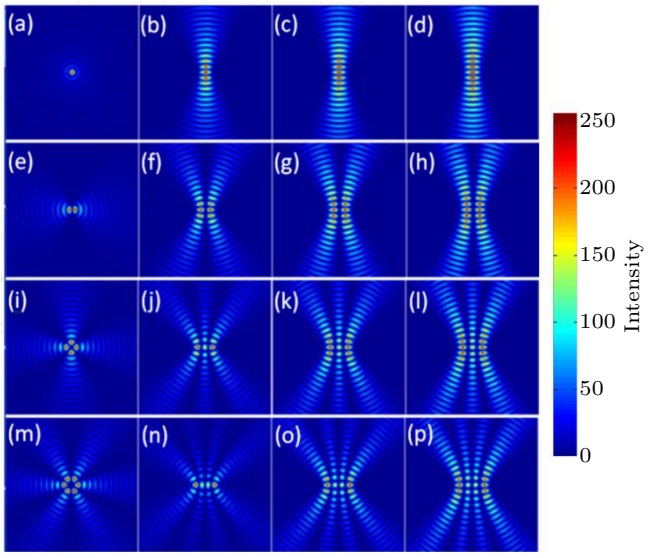


Fig. 1. (color online) Theoretical simulation of even mode Mathieu beams of the first kind in elliptic coordinate. The first to fourth rows represent Mathieu beams for $m = 0$, 1, 2, 3. The first to fourth columns represent the beams for $q = 0$, 15, 30, 45. The red regions represent the crests (maxima intensity of beams), whereas the blue regions represent the valleys (minima intensity of beams).

As shown in Figs. 1(e)–1(p), the transverse intensity pattern distribution of high-order Mathieu beams is fairly complicated. The morphology of high-order Mathieu beams is dependent on the even or odd modes, order number m, and the parameter q of the Mathieu function. Considering the even-parity Mathieu beams for $q = 0$. Figures 1(a), 1(e), 1(i), and 1(m) show that an m-order Mathieu beam has m angular nodal lines over the beam center (m angular valleys over the center of beam); thus $2m$ crests are generated. All Mathieu beams for $q = 0$, including zero-order and high-order Mathieu beams, are axis-symmetry and centrosymmetry beams. Moreover, q is

an important factor to decide the optical distribution of high-order Mathieu beams. When $q = 0$, the radical nodal lines of Mathieu beams are circular, and the crests of high-order Mathieu beam arrays are on a circle. All Mathieu beams for $q \neq 0$ are axis-symmetric beams and not centrosymmetric beams because the radical nodal lines of high-order Mathieu beams are characterized by a set of confocal elliptical and hyperbolic lines and the crests of high-order Mathieu beams array on elliptical and hyperbolic lines. Mathieu functions are the fundamental solutions of wave equation in cylindrical coordinates. With increasing q, the eccentricity of the elliptical and hyperbolic nodal lines of Mathieu beams becomes large. Thus, q is an important parameter that controls the ellipticity of radical nodal lines of Mathieu beams.

In short, Mathieu beams are important diffraction-free beams that have more flexibly and better controllable beam morphology than diffraction-free Bessel and Airy beams, and also for form-invariant Gaussian and Pearcey beams. Hence, precisely generating each types of Mathieu beams is especially valuable and will have wide uses in scientific researches. For example, the optical lattices are theoretically proposed to generate by applying diffraction-free Mathieu beams.[13,14]

3. Experimentation

The history of generating diffraction-free beams started with the experimental setup of Durnin,[1] which demonstrated that the principal properties are derived from Whittaker's solution of Helmholtz equation. The function of $\exp(\cdot)$ is a fundamental solution of Helmholtz equation $(\partial_{xx} + \partial_{yy} + k^2)U = 0$ and describes the transverse field of an ideal plane wave. Any linear superposition of a finite or infinite number of plane waves with the equal wave vector k is a solution of Helmholtz wave equation, which may generate propagation-invariant patterns (*i.e.*, diffraction-free beams).[15] Fundamental diffraction-free optical fields of Helmholtz equation in free space can be written as a superposition of plane waves with a single transverse wave number k_t as follows[4,16]

$$U(x,y,z) = \exp(\mathrm{i}k_z z)\int_0^{2\pi} A(\nu)\exp[\mathrm{i}k_t(x\cos\nu + y\sin\nu)]\,\mathrm{d}\nu, \tag{8}$$

where ν is the angular variable in the radial plane. $A(\nu)$ is the arbitrary complex angular spectrum of the ideal diffraction-free beams. $k_t = k\sin\theta_0$ and $k_z = k\cos\theta_0$ are the radial and axial components of wave vector, respectively. $\theta_0 = \tan^{-1}(R/f_{\mathrm{L}})$ is the angle between the wave vector and beams propagation direction. R is the radius of circle, and f_{L} is the focal length of the Fourier transform lens. Equation (8) represents the superposition of a set of plane waves with same wave vectors. Different spectrum distributions $A(\nu)$ in the circular ring can generate different diffraction-free beams. Mathieu beams are formed as a superposition of fundamental Cosine beams whose mean propagation axes lie on the surface of a cone, and amplitudes are angularly modulated by the angular Mathieu functions.[17]

Equation (8) shows that the several known fundamental solutions of the wave equation that can describe as diffraction-free beams are fully determined by their angular spectrum $A(\nu)$.[18] The function $A(\nu)$ describes the field distribution on the circular ring. From the equation $\theta_0 = \tan^{-1}(R/f_{\mathrm{L}})$, the spectrum parameter is the single radial frequency that is related to both the radius of that circle ring and the focal length of Fourier transform lens. In our case, the focal length f_{L} of the Fourier transform lens is 40 mm. The diffraction-free beams can be understudied as an interference field generated by the coherent superposition of ideal plane waves for a single radial spatial frequency whose relative phase differences remain unchanged upon propagation in the free space.[19] In 1987, diffraction-free Bessel beams were generated by using the setup of annular slit and adding a Fourier transform lens for the case of $A(\nu) = \text{const.}$ to obtain the constant angular spectrum experimentally. Similarly, for the case of $A(\nu) = \mathrm{ce}_m(\nu,q)$ or $\mathrm{se}_m(\nu,q)$, the integral resulting field amplitude is proportional to $\mathrm{Je}_m(u;q)\mathrm{ce}_m(\nu;q)$ or $\mathrm{Jo}_m(u,q)\mathrm{se}_m(\nu,q)$.[4,20] This result implies that the diffraction-free even and odd-parity Mathieu beams can be generated when the amplitudes in the circular ring with radius $R = k_t \cdot f_{\mathrm{L}}$ are modulated by the angular spectrum $\mathrm{ce}_m(\nu,q)\delta(|k| - k_t)$ or $\mathrm{se}_m(\nu,q)\delta(|k| - k_t)$. This distribution of the angular Mathieu spectrum may be difficult to obtain. Therefore, some researchers only approximately generate zero-order Mathieu beams by approximately modulating the annular slit by the angular Mathieu functions.[6,7] In this study, we will precisely modulate the annular distribution of slit by accurately calculating the angular Mathieu functions. We typically calculate any angular transmission distribution of the even type angular Mathieu function of the first kind (*i.e.*, $\mathrm{ce}_m(\nu,q)$) according to the following equation

$$\mathrm{ce}_{2m}(\nu,q) = \sum_{m=0}^{\infty} A_{2k}^{2m}(q)\cos(2k\nu), \tag{9}$$

$$\mathrm{ce}_{2m+1}(\nu,q) = \sum_{m=0}^{\infty} A_{2k+1}^{2m+1}(q)\cos[(2k+1)\nu], \tag{10}$$

the coefficients $A_{2k}^{2m}(q)$ and $A_{2k+1}^{2m+1}(q)$ depend on the parameter q.[4,6,11]

In Durnin's extended experimental setup (see Fig. 2), the angular spectrum is an azimuthally modulated narrow annular pupil with radius $R = 3$ mm and thickness $\Delta R = 80$ μm, as shown in Fig. 3. Mathieu beams can be generated by the complex Fourier-transform of the aperture function. We load the amplitude distribution with angular Mathieu functions in an amplitude-type SLM (GC-SLM-T-XGA, with a

22 μm × 22 μm pitch for each pixel) to generate the transmittance function of a narrow annular pupil $\mathrm{ce}_m(v,q)\delta[(x^2+y^2))-R]$. In the focal plane of the Fourier transform lens, the transverse intensity distributions of several Mathieu beams are recorded using scientific CCD (Microvision 130FC, with a 5.4 μm × 5.4 μm pitch for each pixel), see Fig. 4.

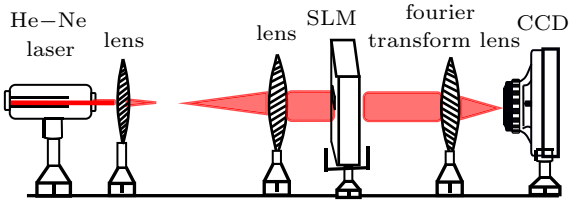


Fig. 2. (color online) The extended experimental setup of Durnin for generating Mathieu beams.

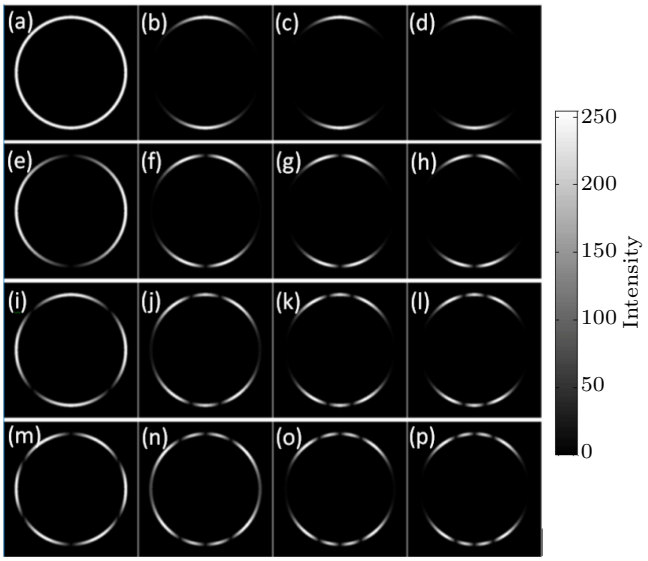


Fig. 3. Narrow annular pupils with angular spectrum that generates Mathieu beams, their parameters being same with those in Fig. 1.

As shown in Fig. 4, we can find that the experimental results agree well with the corresponding numerical results in Fig. 1 if we can eliminate the measurement error induced by the limited resolution of CCD. Moreover, figure 4(a) shows that Bessel beams are the special case of Matheiu beams, which are generated by using a narrow annular pupil modulated by $A(v)=\mathrm{ce}_0(v,0)=1$ as shown in Fig. 3(a). Apparently, it is especially simple case for uniform amplitude over the circular ring. Bessel beams can be regarded as zero-order Mathieu beams for $q=0$.

To show the propagation character of Mathieu beams, we typically record the beams with the parameters $m=0$ and $q=15$ using CCD after the Fourier transform lens. Four output intensity distributions on different transverse planes measured by the CCD are given in Fig. 5. These results clearly demonstrate that the fabricated Mathieu beams can satisfactorily produce the desired diffraction-free beams within a certain range of propagation.

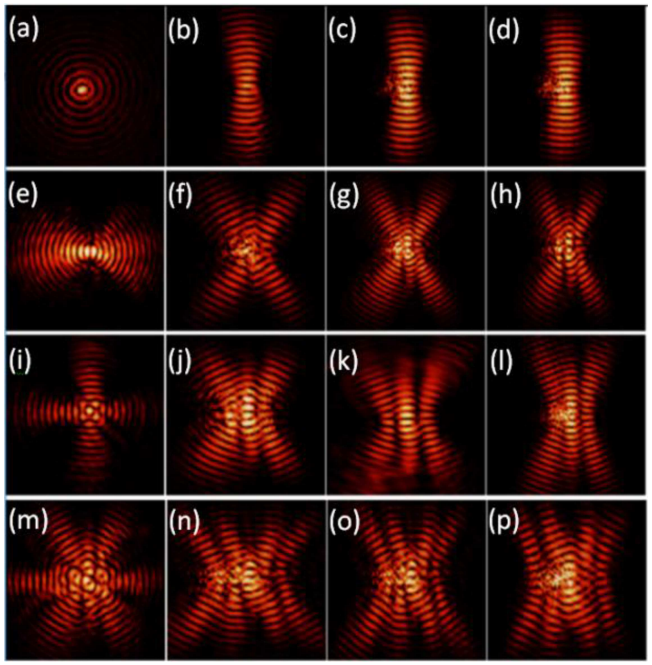


Fig. 4. (color online) Experimentally recording cross-sections of Mathieu beams for the same parameters with those in Fig. 1.

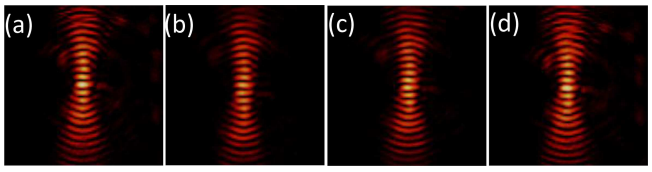


Fig. 5. (color online) The transverse intensity distribution of Mathieu beams for the parameters ($m=0$, $q=15$) at the distance after Fourier transform lens: (a) $z=35$ mm, (b) $z=39$ mm, (c) $z=43$ mm, (d) $z=47$ mm.

4. Conclusions

Using the extended Durnin's experimental setup, we have generated a family of Mathieu beams by spectra amplitude modulation of the incident field using an amplitude-type SLM. As a special case of the Mathieu beams, the Bessel beam is also generated with the same experimental setup. The optical morphology and propagation characteristics of Mathieu beams are also studied. As important diffraction-free beams, Mathieu beams have more flexibility and controllable beam morphology than other known diffraction-free beams. The precise generation of various types of Mathieu beams is expected to lay the foundation for their various applications in both science and technology.

References

[1] Durnin J, Miceli J J, Eberly J H and Diffraction-Free Beams 1987 *Phys. Rev. Lett.* **58** 1499
[2] Lorenser D, Singe C C, Curatolo A and Sampson D D 2014 *Opt. Lett.* **39** 548
[3] Yan Z, Jureller J E, Sweet J, Guffey M J, Pelton M and Scherer N F 2012 *Nano Lett.* **12** 5155
[4] Gutiérrez-Vega J C, Iturbe-Castillo M D and Chávez-Cerda S 2000 *Opt. Lett.* **25** 1493
[5] Wu Q, Ren Z J, Du L Y, Hu H H, Gu Y and Yang Z F 2017 *Acta Phys. Sin.* **66** 204201 (in Chinese)

[6] Gutiérrez-Vega J C, Iturbe-Castillo M D, Ramírez G A, Tepichín E, Rodríguez-Dagnino R M, Chávez-Cerda S and New G H C 2001 *Opt. Commun.* **195** 35
[7] Anguiano-Morales M, Martínez A, Iturbe-Castillo M D and Chávez-Cerda S 2008 *Opt. Commun.* **281** 401
[8] Fahrbach F O, Gurchenkov V, Alessandri K, Nassoy P and Rohrbach A 2013 *Opt. Express* **21** 11425
[9] Bouchal Z 2003 *Czech. J. Phys.* **53** 537
[10] Gutiérrez-Vega J C and Rodríguez-Dagnino R M 2003 *Am. J. Phys.* **71** 233
[11] McLachlan N W 1951 *Theory and Applications of Mathieu Function* (London: Oxford University Press)
[12] Zhang P, Hu Y, Li T, Cannan D, Yin X, Morandotti R, Chen Z and Zhang X 2012 *Phys. Rev. Lett.* **109** 193901
[13] Ye F, Mihalache D and Hu B 2009 *Phys. Rev. A* **79** 053852
[14] Kartashov Y V, Egorov A A, . Vysloukh V A and Torner L 2006 *Opt. Lett.* **31** 238
[15] Kotlyar V V, Kovalev A A and Soifer V A 2014 *Opt. Lett.* **39** 2395
[16] Gutiérrez-Vega J C and Bandres M A 2005 *J. Opt. Soc. Am. A* **22** 289
[17] Alvarez-Elizondo M B, Rodríguez-Masegosa R and Gutiérrez-Vega J C 2008 *Opt. Express* **16** 18770
[18] Bandres M A, Gutiérrez-Vega J C and Chávez-Cerda S 2004 *Opt. Lett.* **29** 44
[19] Dartora C A, Zamboni-Rached M, Nóbrega K Z, Recami E and Hernández-Figueroa H E 2003 *Opt. Commun.* **222** 75
[20] Ruelas A, Lopez-Aguayo S and Gutiérrez-Vega J C 2008 *Opt. Lett.* **33** 2785